

A MECHATRONIC APPROACH TO FULL SHEET CONTROL USING STEER-ABLE NIPS

Rene Sanchez* Edgar Ergueta* Benjamin Fine*
Roberto Horowitz* Masayoshi Tomizuka*
Martin Krucinski**

* *University of California, Berkeley, CA 94720*

** *Xerox Corporation, NY 14580*

Abstract: State of the art high speed color printers require sheets be accurately positioned as they arrive at the image transfer station. To accomplish this goal, a steerable nips mechanism has been designed and built. This mechanism is located upstream from the image transfer station. This steerable nips mechanism allows sheets to be precisely controlled in the longitudinal, lateral, and skew directions. In this paper we present the design, sensing strategy, and a control law based on state feedback linearization. Simulation and experimental results show that the proposed controller is able to correct for paper position errors in the above mentioned directions under the condition that the sheet has nonzero initial and final velocities. The system model is nonlinear and subject to four nonholonomic constraints.

Keywords: Control, nonlinear, nonlinear control system, actuators

1. INTRODUCTION

State of the art paper path control currently requires the sheets to be accurately positioned as they arrive at the image transfer station. This includes correction for longitudinal, lateral, and angular errors. To accomplish this task, current machines have a registration station before the transfer image station. This registration station corrects for lateral and skew errors, and delivers the sheet on time to the image transfer station. State of the art registration devices can not correct for errors at high speeds whereas others mark the paper since they rely on high contact point forces to move the sheet laterally.

In this paper we present a mechatronic solution to full sheet control, which consist on the steer-able nips device depicted in Fig. 1 (US Patent Number 6,634,521) and a control algorithm which permits a swifter correction of lateral errors.

The problem of controlling paper trajectories with steerable nips is similar to the control of two-wheel robots, such as the one studied in (Yun and Sarkar, 1996). However, not only the two-wheel robot has one less degree of freedom, but also the control law proposed in (Yun and Sarkar, 1996) fails to account for singularities that arise when the steering angle of the wheels approach zero. Also, in the case of the two-wheel robot, three inputs are needed to follow a reference trajectory. This is not the case with steerable nips, where four inputs are needed due to the flexibility of the paper, as will be explained shortly.

Similar to the two-wheel robot, the steerable nips mechanism is a nonlinear system with four non-holonomic constraints. Two of these constraints come from the fact that the local velocities (of the paper) in the direction perpendicular to the rotation of the rollers must be zero, and the other two constraints come from non-slip conditions on

these rollers (see Fig. 2). Additional details on the constraints of this particular system can be found in (Sanchez *et al.*, 2004). Furthermore, analytic work related to nonholonomic systems can be found in (Campion *et al.*, 1990), (Campion *et al.*, 1991) and (d’Andrea Novel *et al.*, 1991). The control objective considered here is to move

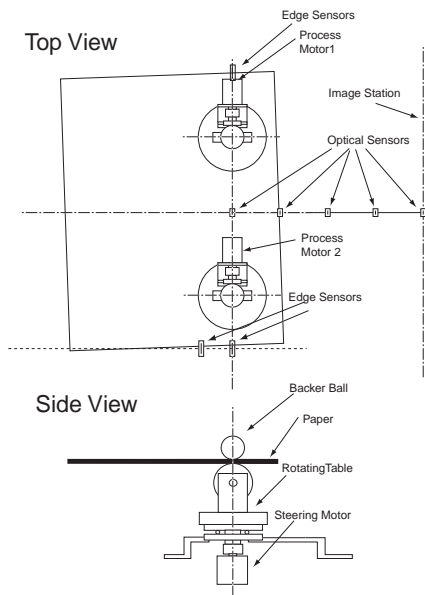


Fig. 1. Schematic of Steerable Nips Fixture

the sheet on the plane from an initial state with nonzero longitudinal velocity to a final state also with nonzero longitudinal velocity, using four inputs; two inputs rotate and steer roller 1, whereas the other two inputs do the same for roller 2 (see Fig. 5). In addition to controlling the lateral, longitudinal, and angular position, this system also controls the amount of paper buckling, δ . A negative δ represents the amount of buckle on a sheet whereas a positive δ occurs when the paper stretches, which needs to be avoided at all times.

To move the sheet from an initial to a final state, the control strategy developed in this paper uses linearization by state feedback (Sasthy, 1999). The control law developed assumes access to the steering angular velocity and the roller’s angular acceleration. In addition, to generate the desired angular acceleration for each roller, a local loop tracks the roller’s desired angular velocity.

The remainder of this paper is organized as follows. Section 2 describes the design of the steerable nips mechanism. The experimental setup is presented in section 3. Section 4 presents the kinematic and dynamic model of the system. The control strategy is derived in section 5. Simulation and experimental results will be shown in section 6. Finally, conclusions and some comments regarding the design and control strategy are stated in section 7.

2. STEERABLE NIPS MECHANISM DESIGN

The steerable nips mechanism is designed so that it can correct for lateral errors without moving the actuator itself. This is achieved by steering two rollers that are in contact with the paper. Thus, sheets can move laterally while they are driven forward. The rollers are also designed to only contact the sheet at a point. This allows the rollers to drive the sheet without inflicting any damage on it. The sheet passes between the roller and a spring loaded backer ball, which can be seen in Fig. 2. The ball provides a normal force, which allows the rollers to drive the sheet.

The roller is driven by a servo motor, which is attached to a rotating table. The table is steered by another servo motor through a coupling as shown in Fig. 2. The roller motors are chosen to be light weight and small to minimize the rotating inertia. For the remaining of this paper the servo motors that drive the rollers will be called *process direction motors* whereas those that steer the rotating table will be called *steering motors*.

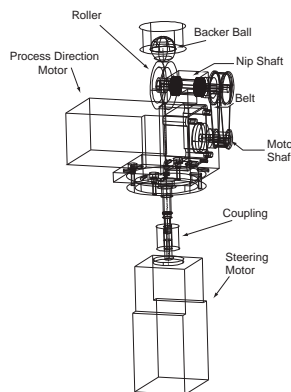


Fig. 2. Process Direction Actuator and Steering Motor Mechanism

3. EXPERIMENTAL SETUP

The experimental setup has been built as shown in Fig. 3. It consists of the following parts:

3.1 Steerable Nips Mechanism

The steerable nips mechanism has been fully described in Section 2; it is located below the horizontal plate shown in Fig. 3. It receives sheets from a feeder unit that was donated by Xerox Corporation. Each of the four motors used for this nips mechanism has an encoder on its shaft for feedback purposes as well as a built-in amplifier. Furthermore, each motor is driven by a PWM signal supplied by the controller board.

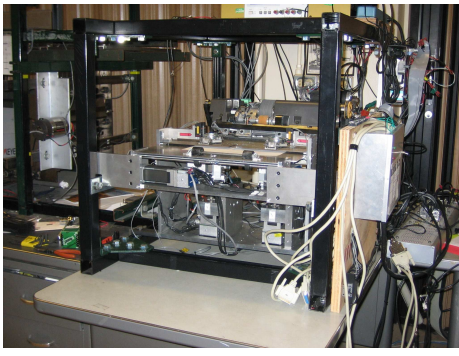


Fig. 3. Experimental Setup

3.2 Exit Roller

An exit roller is designed to remove sheets from the steerable nips mechanism as shown in Fig. 3. This exit roller represents the image transfer station; measuring the paper position and orientation before the exit roller will indicate the controller performance.

3.3 Sensing

Determining the position and orientation of a flexible sheet requires four linear measuring devices. Each sensor must be capable of detecting the paper edge as the paper is moving down the paper path. The current design orients two lateral sensors on the right paper edge and one on the left paper edge. The fourth sensing location is along the process direction. The three lateral sensors detect the paper skew and buckle as shown in Fig. 1.

Current registration uses linear laser sensors for lateral sensing and single photodiodes along the process direction. The lateral sensors measure the position of the paper edge by how much light the sheet blocks between the emitter and sensor. These sensors have a resolution of at least $100 \mu\text{m}$. When the leading paper edge crosses a point sensor, the photodiodes generate an interrupt to the controller software. This signifies that a full paper registration can be made. Five point sensors are located along the process direction spaced 52 mm apart. Estimated sheet longitudinal position between sensors is obtained by an open loop observer.

Another sensing configuration currently being designed improves sensing capabilities along the process direction using less expensive linear optical sensor arrays. Each sensor array consists of 256 photodiodes and can detect the paper edge along the 16.5 mm sensing length to the nearest $64.5 \mu\text{m}$. Eight linear arrays along the process direction provide portions of continuous measurements. Fig. 4 shows the eight process direction sensors. The circuit hardware and printed circuit

boards were designed in-house. Additional circuit hardware measures each of the sensor's 256 photodiodes and provides an eight bit number corresponding to paper edge location to the nearest photodiode. The process direction measurements are transmitted to the controller board (dSpace) serially.

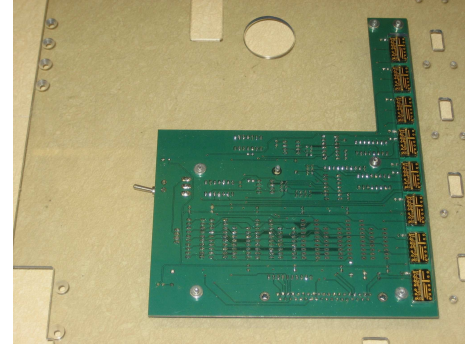


Fig. 4. Process Direction Sensors Using Linear Optical Sensor Arrays

Both sensing configurations have empty gaps along the process direction and thus require the use of observers to estimate the states.

4. KINEMATIC AND DYNAMIC MODEL OF THE STEERABLE NIPS MECHANISM

As it was mentioned in Section 2, the steerable nips mechanism moves a sheet of paper on a flat surface. Fig. 5 represents a sheet position while it is being tracked in the direction of the arrow labeled \underline{v} ; the flat surface is not shown in this figure for clarity purposes. The leading right corner of the sheet, point C , will be used to track the position of the page. Note that while the paper buckles, point C remains on the flat surface since the buckle occurs only between points 1 and 2. For this reason point C does not move perpendicular to the sheet. It is assumed that when the sheet buckles, it is still transversally stiff, making rotation possible. This is illustrated in Fig. 5 where any line perpendicular to the line connecting points 1 and 2 drawn on the buckle surface is parallel to the flat surface.

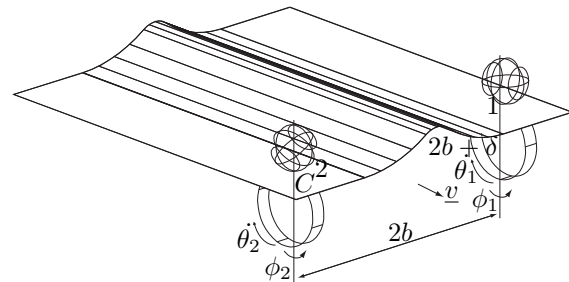


Fig. 5. Steerable Nips with Paper Buckle

4.1 Notation

Figure 6 shows a schematic representation of the model variables for the steerable nips mechanism. This system has two independent steering rollers, located at points 1 and 2. These steerable rollers are separated by a distance $2b$. Three coordinate frames are defined to describe the position and orientation of the paper: A space-fixed coordinate system denoted $(\underline{i}_f, \underline{j}_f, \underline{k}_f)$, and two local frames $(\underline{i}_1, \underline{j}_1, \underline{k}_1)$ and $(\underline{i}_2, \underline{j}_2, \underline{k}_2)$ attached to rollers 1 and 2, respectively. The space-fixed coordinates of the system (x, y, ϕ, δ) locate the leading right corner of the sheet (point C), where x and y are the lateral and longitudinal position, respectively, ϕ is the angular position, and δ is the amount of buckling along the sheet, which is the difference between the distance separating points 1 and 2, as measured along the paper ($2b + \delta$) and along the straight line ($2b$), as shown in Fig. 5. Note that the origin $(0, 0)$ of the space-fixed frame is located in the middle of points 1 and 2. Variables $(\theta_1, \theta_2, \phi_1, \phi_2)$ are coordinates at the actuator level (rollers); θ_1 and θ_2 represent the angular position in the direction parallel to the sheet for rollers 1 and 2, whereas ϕ_1 and ϕ_2 represent the angular position in the direction perpendicular to the sheet for these rollers, respectively.

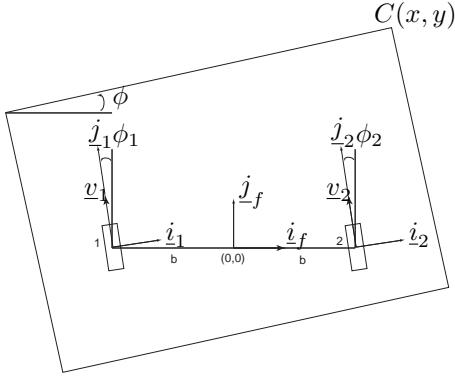


Fig. 6. Schematic of Sheet and Roller from Top

4.2 Kinematics

Using the fixed coordinate frame, the velocities of the paper at points 1 and 2 are

$$\underline{v}_1 = (\dot{x} + \dot{\phi}y)\underline{i}_f + (\dot{y} - \dot{\phi}(x+b))\underline{j}_f \quad (1)$$

$$\underline{v}_2 = (\dot{x} + \dot{\phi}y)\underline{i}_f + (\dot{y} + \dot{\phi}(-x+b+\delta))\underline{j}_f \quad (2)$$

Assuming nonslip conditions for the paper at points 1 and 2 and the fact that the velocities perpendicular to the rollers at the same points are zero (the four nonholonomic constraints mentioned in Section 1), the velocities of the paper

at points 1 and 2 can also be written in local coordinate frames as

$$\underline{v}_1 = -r_1\dot{\theta}_1\underline{j}_1 \quad (3)$$

$$\underline{v}_2 = -r_2\dot{\theta}_2\underline{j}_2 - \dot{\delta}\underline{i}_f \quad (4)$$

where r_1 and r_2 are the radii of rollers 1 and 2, respectively.

Finally, converting the local coordinate frames in Eqs. (3) and (4) to the fixed coordinate frame, and equating terms on each coordinate direction with those in Eqs. (1) and (2), the following kinematic relations can be obtained:

$$\dot{x} = r_1(\sin\phi_1 - \frac{y}{2b+\delta}\cos\phi_1)\dot{\theta}_1 + \frac{r_2y}{2b+\delta}\cos\phi_2\dot{\theta}_2 \quad (5)$$

$$\dot{y} = r_1\cos\phi_1(\frac{x+b}{2b+\delta} - 1)\dot{\theta}_1 - \frac{r_2(x+b)}{2b+\delta}\cos\phi_2\dot{\theta}_2 \quad (6)$$

$$\dot{\phi} = \frac{1}{2b+\delta}(r_1\cos\phi_1\dot{\theta}_1 - r_2\cos\phi_2\dot{\theta}_2) \quad (7)$$

$$\dot{\delta} = r_2\sin\phi_2\dot{\theta}_2 - r_1\sin\phi_1\dot{\theta}_1 \quad (8)$$

These kinematic relations represent the directions of motion where the nonholonomic constraints are satisfied at all times.

4.3 Actuator Dynamics

As can be seen in Fig. 2, the shaft of each process direction motor is connected to the nip's shaft through a belt. The sheet moves due to the force exerted by the nip and backer ball on the page. If we assume that the belt is very stiff and that the motor inductance is very low, we can obtain the following simple model for the process direction actuator dynamics:

$$\ddot{\theta}_i + \alpha_i\dot{\theta}_i = \beta_i V_i \quad (9)$$

where V_i is the voltage input to the motor, and α_i and β_i depend on the inertias and rotational viscous damping coefficients of the different components shown in Fig. 2 as well as on the resistance and torque constants of the motor. The subindexes i ($i = 1$ or 2) correspond to each of the two process direction motors.

4.4 Dynamic System Model

Defining the state vector as $\underline{x} = [x \ y \ \phi \ \delta \ \dot{x} \ \dot{y} \ \dot{\phi} \ \dot{\delta}]^T$, the output vector as $\underline{y} = [x \ y \ \phi \ \delta]^T$, differentiating Eqs.(5)-(8), and using Eq. (9) for both process direction motors, we obtain the following dynamic model:

$$\ddot{\underline{y}} = m(\underline{x}) + N(\underline{x}) \begin{bmatrix} \ddot{\theta}_1 \\ \ddot{\theta}_2 \\ \dot{\phi}_1 \\ \dot{\phi}_2 \end{bmatrix} \quad (10)$$

$$\begin{aligned} \ddot{\theta}_1 + \alpha_1 \dot{\theta}_1 &= \beta_1 u_1 \\ \ddot{\theta}_2 + \alpha_2 \dot{\theta}_2 &= \beta_2 u_2 \\ \dot{\phi}_1 &= u_3 \\ \dot{\phi}_2 &= u_4 \end{aligned}$$

where $m(\underline{x})$ is a 4×1 vector and $N(\underline{x})$ is a 4×4 matrix. Note in Eq.(10) that the input voltages to the process motors are two of the four system inputs; we call them u_1 and u_2 . The other two inputs, u_3 and u_4 , are the steering angular velocities. For simplicity, we have assumed that local velocity feedback control is applied to each of the two steering motors such that the motor speeds may be regarded as the control inputs.

5. CONTROL STRATEGY

The block diagram of the control system is shown in Fig. 7. The nonlinear feedback law, C_{FBL} ,

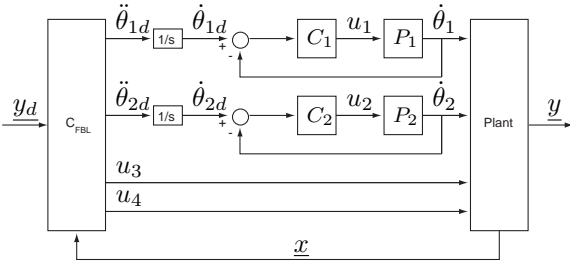


Fig. 7. Control System Block Diagram

is based on feedback linearization (Slotine and Li, 1991):

$$\begin{bmatrix} \ddot{\theta}_{1d} \\ \ddot{\theta}_{2d} \\ u_3 \\ u_4 \end{bmatrix} = N^{-1}(\underline{x})(\underline{v} - m(\underline{x})) \quad (11)$$

Whereas two of the inputs to the plant are obtained directly from the feedback linearization control law, the other two are generated by first integrating the signals $\ddot{\theta}_{1d}$ and $\ddot{\theta}_{2d}$ and then controlling the angular velocities of the motors using simple integral control ($C_1(s)$ and $C_2(s)$ in Fig.(7)). Furthermore, choosing

$$\begin{bmatrix} v_1 \\ v_2 \\ v_3 \\ v_4 \end{bmatrix} = \begin{bmatrix} \ddot{x}_d + k_1 \dot{\tilde{x}} + q_1 \tilde{x} \\ \ddot{y}_d + k_2 \dot{\tilde{y}} + q_2 \tilde{y} \\ \ddot{\phi}_d + k_3 \dot{\tilde{\phi}} + q_3 \tilde{\phi} \\ \ddot{\delta}_d + k_4 \dot{\tilde{\delta}} + q_4 \tilde{\delta} \end{bmatrix}$$

with $k_i, q_i > 0$ for $i=1,2,3,4$ gives exponentially decreasing errors for each of the output variables, provided that matrix $N^{-1}(\underline{x})$ is not ill conditioned. The inverse of matrix $N(\underline{x})$ is:

$$N(\underline{x})^{-1} = \begin{bmatrix} n_{i11} & n_{i12} & n_{i13} & n_{i14} \\ n_{i21} & n_{i22} & n_{i23} & n_{i24} \\ n_{i31} & n_{i32} & n_{i33} & n_{i34} \\ n_{i41} & n_{i42} & n_{i43} & n_{i44} \end{bmatrix}, \quad (12)$$

with

$$\begin{aligned} n_{i11} &= \frac{\dot{x} + y\dot{\phi}}{d_1} \\ n_{i12} &= \frac{-\dot{y} + (b+x)\dot{\phi}}{d_1} \\ n_{i13} &= \frac{\dot{x}y - \dot{y}(b+x) + \dot{\phi}(b^2 + 2bx + x^2 + y^2)}{d_1} \\ n_{i14} &= 0 \\ n_{i21} &= \frac{\dot{x} + \dot{\delta} + y\dot{\phi}}{d_2} \\ n_{i22} &= \frac{-\dot{y} - (b-x+\delta)\dot{\phi}}{d_2} \\ n_{i23} &= \frac{\dot{x}y + \dot{\delta}y + \dot{y}(b-x+\delta) + (y^2 + (b-x+\delta)^2)\dot{\phi}}{d_2} \\ n_{i24} &= \frac{\dot{x} + \dot{\delta} + y\dot{\phi}}{d_2} \\ n_{i31} &= \frac{-\dot{y} + (b+x)\dot{\phi}}{d_3} \\ n_{i32} &= \frac{\dot{x} + y\dot{\phi}}{d_3} \\ n_{i33} &= \frac{b\dot{x} + x\dot{x} + y\dot{y}}{d_3} \\ n_{i34} &= 0 \\ n_{i41} &= \frac{\dot{y} + (b-x+\delta)\dot{\phi}}{d_4} \\ n_{i42} &= \frac{\dot{x} + \dot{\delta} + y\dot{\phi}}{d_4} \\ n_{i43} &= \frac{-y\dot{y} + (\delta + b - x)\dot{x} + (\delta + b - x)\dot{\delta}}{d_4} \\ n_{i44} &= \frac{\dot{y} + (b-x+\delta)\dot{\phi}}{d_4} \end{aligned}$$

and

$$\begin{aligned} d_1 &= r_1 \sqrt{(-\dot{y} + (b+x)\dot{\phi})^2 + (\dot{x} + y\dot{\phi})^2} \\ d_2 &= r_2 \sqrt{(\dot{x} + \dot{\delta} + y\dot{\phi})^2 + (-\dot{y} - (b-x+\delta)\dot{\phi})^2} \\ d_3 &= (-\dot{y} + (b+x)\dot{\phi})^2 + (\dot{x} + \dot{\delta} + y\dot{\phi})^2 \\ d_4 &= (\dot{y} + (b-x+\delta)\dot{\phi})^2 + (\dot{x} + \dot{\delta} + y\dot{\phi})^2 \end{aligned}$$

Looking at the elements of matrix $N^{-1}(\underline{x})$, we can see that this matrix will not be ill conditioned if $d_i \neq 0$, for $i = 1, 2, 3, 4$. It can be shown that this condition is satisfied as long as the sheet is moving. The proof for local stability has not been included in this manuscript because of constraints on the number of pages. It should also be noted that, for the nonlinear part of the system, since the relative degree of the system in Eq.10 is 8, and vector \underline{x} has 8 states, there are no internal dynamics on the linearization.

6. SIMULATION AND EXPERIMENTAL RESULTS

The system model given by Eq. (10) was simulated to go from an initial state of $(x, y, \phi, \delta, \dot{x}, \dot{y}, \dot{\phi}, \dot{\delta}) = (-5.31mm, 49.1mm, -0.8^\circ, 0, 0, 500mm/sec, 0, 0)$ to a final state of $(x, y, \phi, \delta, \dot{x}, \dot{y}, \dot{\phi}, \dot{\delta}) = (0, 0.5t, 0, 0, 0, 500mm/sec, 0, 0)$. The variable t stands for time in seconds since the desired longitudinal trajectory is a ramp. The following values for the nonlinear control gains were used: $k_1 = k_2 = k_3 = k_4 =$

30, $q_1 = q_2 = q_3 = q_4 = 205$. The simulation and experimental results for the paper states can be seen in Fig. 8 and Fig. 9. The dotted lines in these two figures represent the simulated results and the solid lines are the experimental results. The time axes in the experimental results were shifted to match with the simulated results. Note that the four position variables were controlled in less than 0.3 seconds. The discrepancies between the simulation and experimental results are small and they can be attributed to sensor noise and sensor accuracy. Discrepancies between experimental and simulated results of paper buckle can also be attributed to paper slip, since buckle (δ) is obtained by integrating Eq. (8).

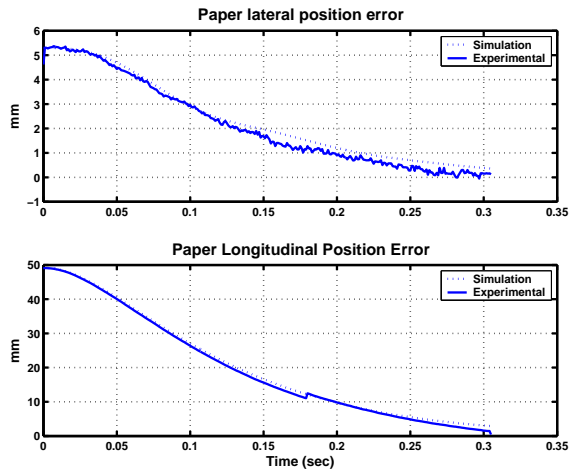


Fig. 8. Paper Longitudinal and Lateral Position Errors

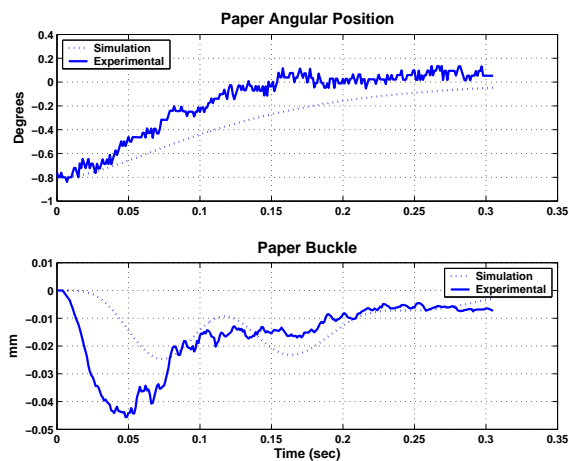


Fig. 9. Paper Angular Position and Buckle

7. CONCLUSION

In this paper we have presented an innovative design that permits a swifter correction of lateral and orientation errors in a paper path control system for xerographic and printing devices. This mechanism accomplished this task by having steerable nips.

The proposed controller was obtained by state feedback linearization (Sastry, 1999). Simulation and experimental results obtained in this paper have shown that, by using the proposed control strategy, it is possible to drive a sheet from an initial state with nonzero longitudinal velocity to a final state also with nonzero longitudinal velocity in a very short time. This is accomplished without violating the nonholonomic constraints.

In the near future we expect to present experimental results of different control strategies. Also, for practical reasons, we will develop a nonlinear observer and different control laws that allow us to control paper with limited sensing in the longitudinal direction.

8. ACKNOWLEDGEMENTS

This work was supported by the National Science Foundation under Grant CMS 0301719 and by financial support and collaboration from Xerox Corporation.

REFERENCES

- Campion, G., B. d'Andrea Novel and G. Bastin (1991). Modelling and state feedback control of nonholonomic mechanical systems. In: *Proceedings of the 30th IEEE Conference on Decision and Control*. Brighton, England. pp. 1184–1189.
- Campion, G., d'Andrea Novel and G. Bastin (1990). Controllability and state feedback stabilisability of nonholonomic mechanical systems. In: *Advanced robot control : proceedings of the International Workshop on Nonlinear and Adaptive Control: Issues in Robotics*. Grenoble. pp. 106–124.
- d'Andrea Novel, B., G. Bastin and G. Campion (1991). Modelling and control of nonholonomic wheeled mobile robots. In: *Proceedings of the 1991 IEEE Conference on Robotics and Automation*. Sacramento, CA. pp. 1130–1135.
- Sanchez, Rene, Roberto Horowitz and Masayoshi Tomizuka (2004). Paper sheet control using steerable nips. In: *2004 American Control Conference Proceedings*. Boston, Massachusetts. pp. 482–487.
- Sastry, S. S. (1999). *Nonlinear Systems : Analysis, Stability, and Control*. Springer.
- Slotine, J.-J. E. and W. Li (1991). *Applied Nonlinear Control*. Prentice Hall, Inc.. N.J.
- Yun, Xiaoping and N. Sarkar (1996). Dynamic feedback control of vehicles with two steerable wheels. In: *1996 IEEE International Conference on Robotics and Automation*. pp. 3105–3110.